

COMPUTER SIMULATION OF POSITIVE STREAMER DYNAMICS IN UNIFORM AND NON-UNIFORM ELECTRIC FIELDS IN AIR

O.V. Manuilenko

National Science Center "Kharkov Institute of Physics and Technology", Kharkov, Ukraine

E-mail: ovm@kipt.kharkov.ua

The results of numerical simulations of the propagation of a positive streamer in air in the uniform and strongly non - uniform electric fields are presented. It is shown that the dynamics of the streamer propagation in air retains the main features characteristic of a negative streamer in nitrogen. It is shown that the velocity of the streamer in a non - uniform electric field is higher than its velocity in an uniform field at given voltages on electrodes. It is shown that with decreasing needle radius the velocity of the streamer is increased at given voltages on electrodes. This growth continues until a critical radius, after which the growth of the positive streamer velocity practically stops.

PACS: 52.80.Mg, 52.80.Tn

INTRODUCTION

Papers [1 - 7] are devoted to the numerical modeling of the positive (cathode-directed) streamer in air within the drift-diffusion approximation. These works are used both structured and unstructured meshes to solve the continuity and Poisson equations. Streamer is a nonlinear structure with a sharp edge. Therefore, for its correct resolution in numerical simulations were used the exponential representation for the current density in the drift-diffusion approximation – the Scharfetter-Gummel algorithm [8], or flux – corrected transport schemes [9]. In [1 - 7], for different values of the applied voltage, different radii of curvature of the needle, and different distances between the electrodes, the velocity of the streamer obtained in the range of $10^7 \dots 10^8$ cm/s, which is in good agreement with experiment. A systematic study of the influence of radius of the needle on the speed of the positive streamer is not conducted. This is the subject of the paper.

The computer simulations of the negative (anode - directed) streamers in nitrogen in the uniform (plane - to - plane geometry) and non - uniform (needle - to - plane geometry) fields are presented in [10, 11]. It is shown that the behavior of the streamer velocity versus time has four specific regions: a sharp drop at the beginning of the movement, a propagation with a constant velocity, an area of the first (low) acceleration, and a region of the second (strong) acceleration at the approach of the streamer head to an anode. It is shown that the velocity of the negative streamer in a non - uniform electric field is always higher than its velocity in an uniform field at the same potentials on the electrodes. It is shown in [11] that with decreasing radius of the needle, the streamer velocity is increased. The growth of the streamer speed, with decreasing of the needle radius, is stopped when the needle curvature radius reaches a certain critical size.

Below the results of numerical simulations, using the finite element method (SUPG, CWDPG), of positive streamer dynamics in air are presented. The computer simulations have been performed for uniform and for non - uniform electric fields. It is shown that the dynamics of the streamer propagation in air retains the main features characteristic of a negative streamer in nitrogen.

1. MODEL

The coupled continuity equations for electrons, positive ions, negative ions, and Poisson equation for simulation of positive streamer dynamics in air are:

$$\frac{\partial n_e}{\partial t} + \nabla \cdot (\vec{\Gamma}_e) = S_{iz} + S_{ph} - S_{att} - L_{ep}, \quad (1)$$

$$\frac{\partial n_p}{\partial t} = S_{iz} + S_{ph} - L_{ep} - L_{pn}, \quad (2)$$

$$\frac{\partial n_n}{\partial t} = S_{att} - L_{pn}, \quad (3)$$

$$\nabla^2 V = -\rho / \epsilon_0, \quad (4)$$

where n_e , n_p , n_n are the number densities for electrons, positive ions and negative ions, $\vec{\Gamma}_e = -n_e \mu_e \vec{E} - D_e \nabla n_e$ is the electron flux in the drift-diffusion approximation, μ_e , D_e are the electron mobility and diffusion coefficients, V is the potential of the electric field, $\vec{E} = -\nabla V$, $\rho = e(n_p - n_e - n_n)$, e is the electron charge, ϵ_0 is the permittivity of free space. In Eqs. (1) - (3), S and L stand for sources and losses of charged particles. S_{iz} is the rate of charged particle generation due to collisional ionization, S_{ph} is the rate of photoionization, S_{att} is the rate of electron attachment, L_{ep} is the rate of electron-ion recombination, and L_{pn} is the rate of ion-ion recombination. Ions in (2), (3) are considered as immovable since their mobility several orders of magnitude smaller than the electron mobility, which allows, for the simulation time, neglect their displacement. In the calculations was used a set of transport coefficients and rate constants given in [12, 13]. The rate of photoionization in air is [14]:

$$S_{ph}(\vec{r}) = \int_{V'} I(\vec{r}') g(R) / 4\pi R^2 dV', \quad (5)$$

where $R = |\vec{r} - \vec{r}'|$, $I(\vec{r}') = \xi S_{iz}(\vec{r}') p_q / (p + p_q)$,

$$g(R) = \frac{\exp(-\chi_{\min} p_{O_2} R) - \exp(-\chi_{\max} p_{O_2} R)}{R \ln(\chi_{\max} / \chi_{\min})}. \quad \text{Here}$$

$\xi = 0.1$, $p_q = 30$ Torr, p is the total pressure of the gas mixture, $\chi_{\min} = 3.5 \cdot 10^{-2} \text{ cm}^{-1} \text{ Torr}^{-1}$, $\chi_{\max} = 2.0 \text{ cm}^{-1} \cdot \text{Torr}^{-1}$.

Fig. 1 shows the simulation domain and boundary conditions. Initially electrons and ions are located at the anode with number densities:

$n_{e,p,n} = \delta_{e,p,n} \exp(-r^2/\sigma_r - (z-L_z)^2/\sigma_z)$, $\delta_e = 9 \cdot 10^{13} \text{ cm}^{-3}$, $\delta_p = 1 \cdot 10^{14} \text{ cm}^{-3}$, $\delta_n = 1 \cdot 10^{13} \text{ cm}^{-3}$, $\sigma_r = 1 \cdot 10^{-4} \text{ cm}^2$, $\sigma_z = 6.25 \cdot 10^{-4} \text{ cm}^2$. Anode voltage is $V_0 = 8 \text{ kV}$, $L_z = 0.2 \text{ cm}$, $L_r = 0.05 \text{ cm}$, needle radius is one of $R = \{0.25, 0.5, 1.0, 2.0\} \cdot H_{ndl}$, needle height is $H_{ndl} = 0.3125 \text{ mm}$. In the case of plane - to - plane geometry $R + H_{ndl} = 0$.

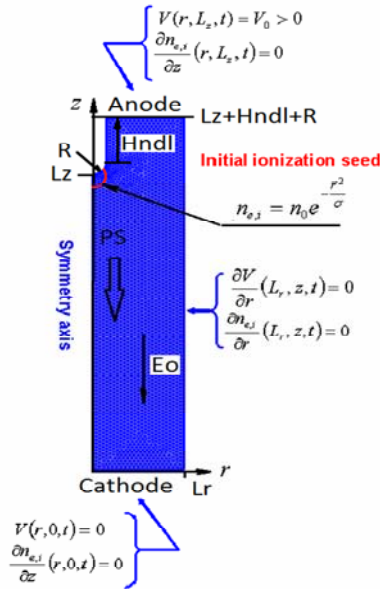


Fig. 1. Simulation domain and boundary conditions

2. UNIFORM ELECTRIC FIELDS

Figs. 2, 3 show the dynamics of positive streamer in the homogeneous fields. The initial conditions are chosen to avoid the avalanche stage, when the Laplacian electric field is not disturbed by the field of the generated space charge field - $\delta_{e,p} \propto 10^{14} \text{ cm}^{-3}$.

Fig. 2 shows distribution of the space charge density $\rho(r, z; t)$ in $\{r, z\}$ at different times. Fig. 3 presents the distribution of the absolute value of the electric field $|\vec{E}(r, z; t)|$ at the same time points. The arrows in Figs. 2 and 3 show the electric field $\vec{E}(r, z; t)$. After a short initial stage ($< 1 \cdot 10^{-10} \text{ s}$), a positive streamer is formed. It moves in the direction of the applied Laplacian field. For $t > 1 \cdot 10^{-9} \text{ s}$ the electric field is substantially enhanced in front of the streamer head, and attenuated behind it. After an initial rise, the electric field in front of the streamer head slightly decreases as it moves toward the cathode. It is clear from Fig. 2 that after the formation of the streamer head, the radius first decreases and then increases as it moves to the cathode, creating a constriction on the body of the streamer.

Fig. 4 shows the distributions in $\{r, z\}$ of the impact ionization rate $S_{iz}(r, z; t)$ at different times, and the corresponding distributions of the photoionization rate $S_{ph}(r, z; t)$. It is clear from Fig. 4 that the generation of the electrons due to photoionization has a maximum

in the vicinity of the streamer head, where is maximal impact ionization. The photoionization region is always wider than the area of impact ionization, which leads to the birth of the electrons in front of the positive streamer head, and is one of the conditions of its movement.

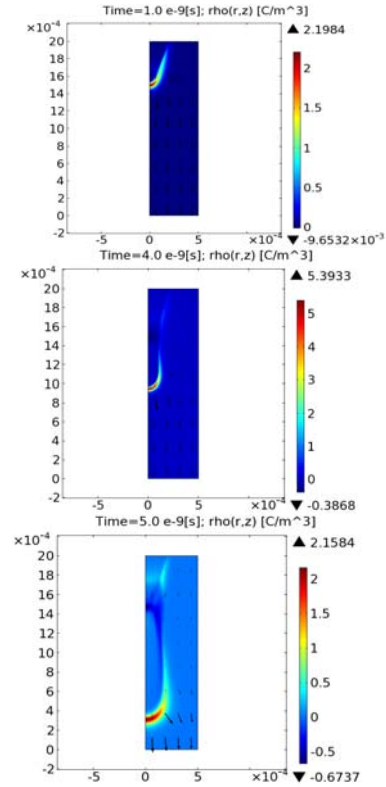


Fig. 2. Space charge density $\rho(r, z; t)$

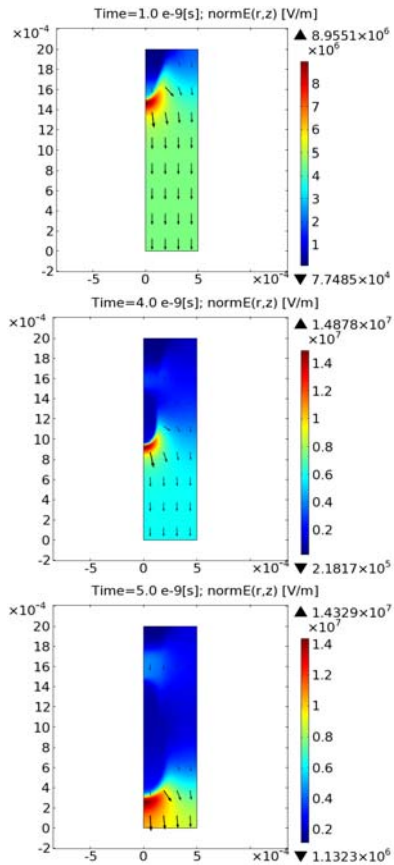


Fig. 3. Absolute value of the electric field $|\vec{E}(r, z; t)|$

Fig. 5 shows the space charge density $\rho(r=0, z; t)$ and the absolute value of the electric field $|\vec{E}(r=0, z; t)|$ on the axis at different times during the movement of the streamer. After a rapid rise in the initial stage, the space charge density $\rho(r=0, z; t)$ and the electric field $|\vec{E}(r=0, z; t)|$ at the streamer head decrease. When the head of the streamer approaches the cathode, the local electric field in front of the streamer head is increased. This leads to the growing impact ionization rate and the rate of photoionization. This, in turn, leads to an increase in the densities of charged particles, and the rise of the space charge density $\rho(r=0, z; t)$.

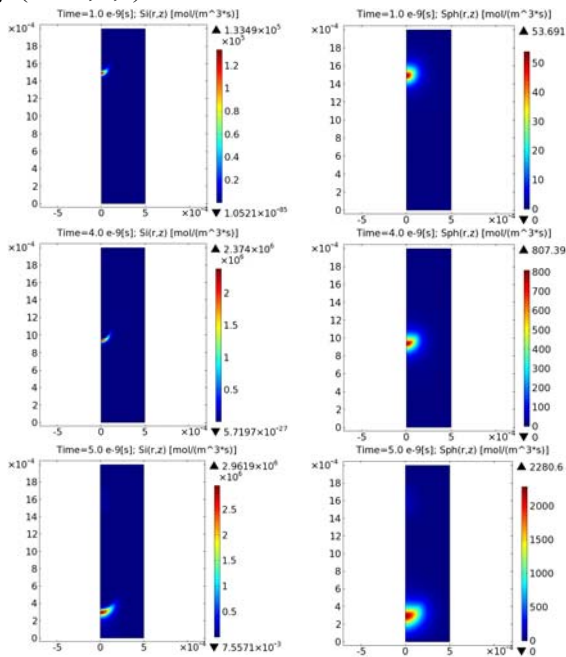


Fig. 4. Left column - $S_{iz}(r, z; t)$.

Right column - $S_{ph}(r, z; t)$

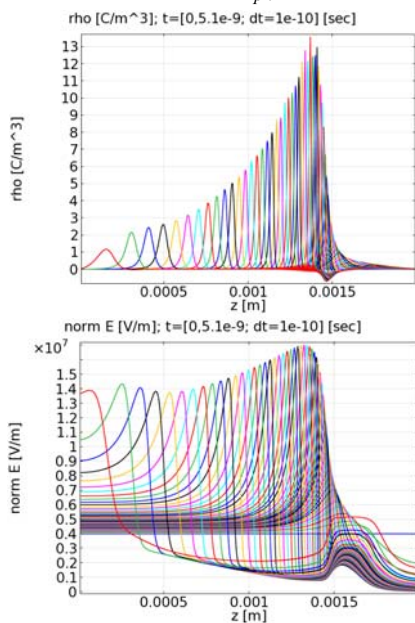


Fig. 5. Space charge density $\rho(r=0, z; t)$ and electric field $|\vec{E}(r=0, z; t)|$ on the axis at different times

As the streamer moves to the cathode, the positive streamer head is broadened in the longitudinal direction, which is associated with the presence of photoionization. It is clearly seen from the space charge density distributions on the axis at different times (see Fig. 5). This behavior differs from the movement of the negative streamer in nitrogen, where there is no photoionization, and the head of the negative streamer, as it moves towards the anode, shrinks and increases in magnitude.

Fig. 6 shows the z -coordinate of the maximum of the electric field $|\vec{E}(r=0, z; t)|^{\max}$ on the axis versus time, and the velocity of $|\vec{E}(r=0, z; t)|^{\max}$ versus time, which is the positive streamer propagation velocity through the discharge gap - $V_s(t)$.

The behavior of this velocity has, as in the case of the negative streamer in nitrogen [11], the characteristic regions: (1) the sharp drop of the velocity at the beginning of the movement, (2) the propagation with a constant velocity, (3) the area of the first (low) acceleration, and (4) the region of the second (strong) acceleration at the approach of the streamer head to the cathode. In contrast to the negative streamer in nitrogen [11], the region of constant velocity can not be identified as the initial linear stage of the avalanche development, when the space charge is small, and the external electric field is practically not distorted by the space charge.

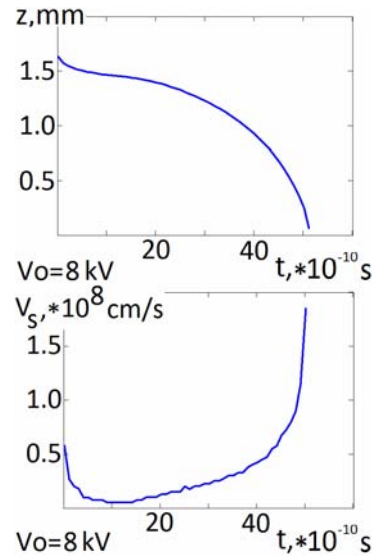


Fig. 6. z -coordinate of the maximum of the electric field $|\vec{E}(r=0, z; t)|^{\max}$ on the axis versus time, and streamer velocity $V_s(t)$ versus time

3. NON-UNIFORM ELECTRIC FIELDS

Figs. 7, 8 show, as an example, the simulation results of the positive streamer propagation through the discharge gap with non-uniform electric fields. $V_0 = 8$ kV, $R = 1.0$ -Hndl. The initial and boundary conditions are the same as in Section 3. Fig. 7 presents the space charge density $\rho(r, z; t)$ at different time points. Fig. 8 shows the absolute value of the electric field $|\vec{E}(r, z; t)|$ at the same time points. The arrows indicate the electric field.

The dynamics of the streamer passage through the discharge gap is changed in comparison with the case of the uniform field. These changes are due to increased vacuum (Laplacian) electric field on the needle and the appearance of the radial electric field. The increased Laplacian electric field on the tip causes movement of the streamer, at least at the initial stage, in higher fields as compared with the plane - to - plane case. Which in turn, leads to an increase in its speed (see also Figs. 9, 10), and a decrease the time of the streamer formation. The radial electric field increases the transverse dimension of the streamer in comparison with the plane - to - plane case.

After a short initial stage ($< 1 \cdot 10^{-10}$ s), a positive streamer is formed. For $t > 1 \cdot 10^{-9}$ s the electric field is enhanced in front of the positive streamer head, and attenuated behind it.

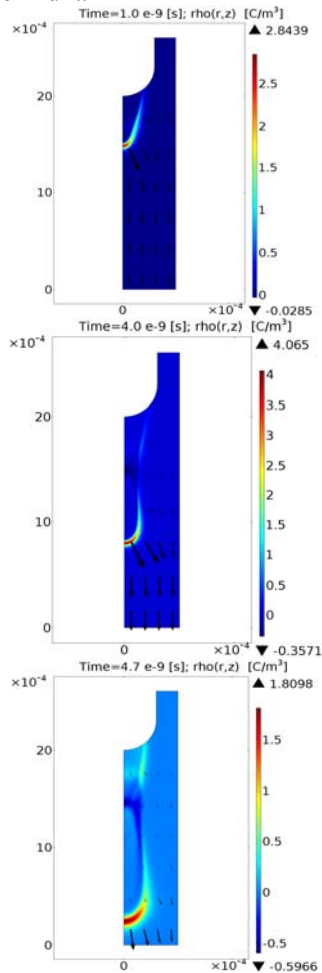


Fig. 7. Space charge density $\rho(r, z; t)$

After an initial growth, the electric field in front of the streamer head decreases as it moves through the discharge gap, and then increases when the head of streamer comes close to the cathode. It is clear from Fig. 7 that after the formation of the streamer head, the radius first decreases and then increases as it moves to the cathode, creating a constriction on the body of the streamer. As in the plane case, the generation of the electrons due to photoionization has a maximum in the vicinity of the streamer head, where is maximal impact ionization. Photoionization region is always wider than the area of impact ionization, which leads to the birth of the electrons in front of the positive streamer head.

Fig. 9 shows the z -coordinates of the maximum of the electric field $|\vec{E}(r = 0, z; t)|^{\max}$ on the axis as function of time, and velocities of the positive streamers $V_s(t)$ for different values of the radii of the needle $R = \{0.25, 0.5, 1.0, 2.0, \text{inf}\} \cdot H_{ndl}$ at anode potential $V_0 = 8$ kV. The $R = \text{inf}$ means uniform electric field, or plane - to - plane computational domain.

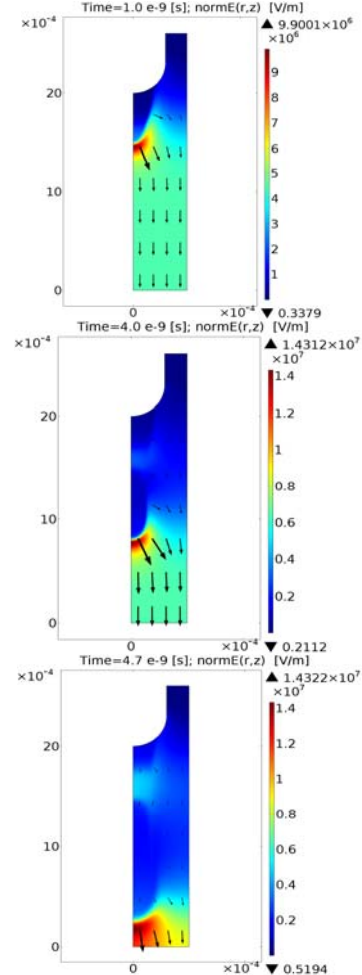


Fig. 8. Absolute value of the electric field $|\vec{E}(r, z; t)|$

As seen from Fig. 9, the velocity of the positive streamer versus time $V_s(t)$ behaves as a speed of the negative streamer in nitrogen [11]. There are four characteristic regions: (1) the sharp drop of the velocity at the beginning of the movement, (2) the propagation with a constant velocity, (3) the area of the first (weak) acceleration, and (4) the region of the second (strong) acceleration at the approach of the streamer head to the cathode. As seen from Fig. 9, the streamer velocity increases with decreasing radius of curvature of the needle at a predetermined potential on the anode. This increase in the velocity goes up to a certain radius (in this case $R = 0.5 \cdot H_{ndl}$), after which the growth of the streamer speed is cutted off.

Fig. 10 shows the streamer mean velocity $\langle V_s \rangle$ as a function of the needle radius. Mean velocity is defined as $\langle V_s \rangle = L_z / \tau_{tr}$, where L_z is the discharge gap length, τ_{tr} is the passage time of the streamer through the discharge gap. The dashed line in Fig. 10 shows the

speed $\langle V_s \rangle$ for uniform field. It can be seen that the $\langle V_s \rangle$ increases with decreasing R . Starting from some R , the growth of the speed stops. It is also seen that the velocity in a non - uniform field is higher than the speed in an uniform field.

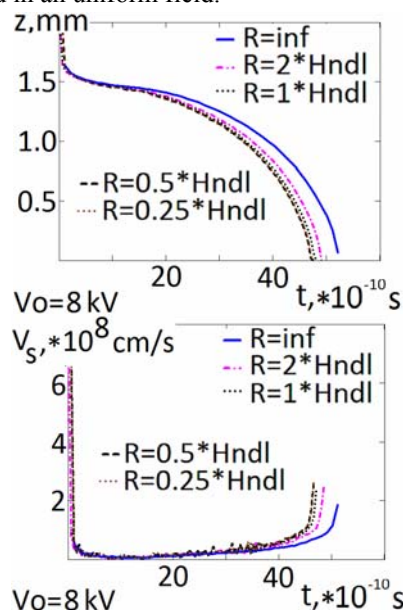


Fig. 9. Positive streamer dynamics for different radii of the needle $R = \{0.25, 0.5, 1.0, 2.0, \text{inf}\} \cdot H_{ndl}$. Applied voltage $V_0 = 8 \text{ kV}$. $H_{ndl} = 0.3125 \text{ mm}$. Top - z-coordinate of the maximum of the electric field $|\vec{E}(r = 0, z; t)|^{\text{max}}$ on the axis versus time. Bottom - streamer velocity $V_s(t)$ versus time

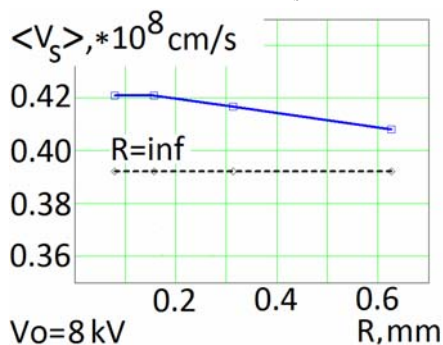


Fig. 10. The dependence of the positive streamer average speed $\langle V_s \rangle$ on the radius of the needle $R = \{0.25, 0.5, 1.0, 2.0, \text{inf}\} \cdot H_{ndl}$ for applied voltage $V_0 = 8 \text{ kV}$. $H_{ndl} = 0.3125 \text{ mm}$

CONCLUSIONS

The results of numerical simulations of the propagation of a positive streamer in the atmospheric pressure air in the uniform and strongly non - uniform electric fields are presented. It is shown that the velocity of the positive streamer versus time behaves as a speed of the negative streamer in nitrogen [11]. There are four characteristic regions: the sharp drop of the velocity at the beginning of the movement, the propagation with a nearly constant velocity, the area of the first (low) acceleration, and the region of the second (strong) acceleration at the approach of the streamer head to the cathode.

It is shown that the propagation velocity of the positive streamer in a non - uniform electric field is higher than its velocity in an uniform field at given voltages on electrodes.

It is shown that with decreasing needle radius velocity of the streamer is increased at given voltages on electrodes. This growth continues until a critical radius, after which the growth of the positive streamer velocity practically stops.

REFERENCES

1. A.A. Kulikovskiy. Two-dimensional simulation of the positive streamer in N2 between parallel-plate electrodes // *J. Phys. D: Appl. Phys.* 1995, v. 28, p. 2483-2493.
2. R. Morrow, J.J. Lowke. Streamer propagation in air // *J. Phys. D: Appl. Phys.* 1997, v. 30, p. 614-627.
3. N.Y. Babaeva, G.V. Naidis. Two-dimensional modelling of positive streamer dynamics in non - uniform electric fields in air // *J. Phys. D: Appl. Phys.* 1996, v. 29, p. 2423-2431.
4. A.A. Kulikovskiy. Positive streamer in a weak field in air: A moving avalanche-to-streamer transition // *Phys. Rev.* 1998, v. 57, p. 7066-7074.
5. A.A. Kulikovskiy. The role of photoionization in positive streamer dynamics // *J. Phys. D: Appl. Phys.* 2000, v. 33, p. 1514-1524.
6. G.E. Georghiou, R. Morrow, A.C. Metaxas. Two-dimensional simulation of streamers using the FE-FCT algorithm // *J. Phys. D: Appl. Phys.* 2000, v. 33, p. L27-L32.
7. A. Luque, V. Ratushnaya, U. Ebert. Positive and negative streamers in ambient air: modeling evolution and velocities // *J. Phys. D: Appl. Phys.* 2008, v. 41, p. 234005-234017.
8. A.A. Kulikovskiy. A more accurate Scharfetter-Gummel algorithm of electron transport for semiconductor and gas discharge simulation // *J. Comp. Phys.* 1994, v. 119, p. 149-155.
9. J.P. Boris, D.L. Book. Solution of continuity equations by the method of flux-corrected transport // *Methods in computational physics.* 1976, v. 16, p. 85-129.
10. V.I. Golota, Yu.V. Dotsenko, V.I. Karas', O.V. Manuilenko, A.S. Pismenetskii. Simulation of negative streamer in nitrogen // *Problems of Atomic Science and Technology. Ser. «Plasma Electronics and New Meth. of Accel.»* (7). 2010, № 4, p. 176-180.
11. O.V. Manuilenko, V.I. Golota. Particularities of the negative streamer propagation in homogeneous and inhomogeneous electric fields // *Problems of Atomic Science and Technology. Ser. «Plasma Physics»* (83). 2013, № 1, p. 171-173.
12. A.A. Kulikovskiy. Positive streamer between parallel plate electrodes in atmospheric pressure air // *J. Phys. D: Appl. Phys.* 1997, v. 30, p. 441-450.
13. R.S. Sigmond. The residual streamer channel: return strokes and secondary streamers // *J. Appl. Phys.* 1984, v. 56, p. 1355-1370.
14. M.B. Zheleznyak, A.Kh. Mnatsakanian, S.V. Szykh. Fotoionizatsiya smecy azota i kisloroda izlucheniem gazovogo razryada // *Teplofizika Vysokih Temp.* 1982, v. 20, p. 423-428 (in Russian).

Article received 29.04.2013.

ISSN 1562-6016. BAHT. 2013. №4(86)

ЧИСЛЕННОЕ МОДЕЛИРОВАНИЕ ДИНАМИКИ ПОЛОЖИТЕЛЬНОГО СТРИМЕРА В ОДНОРОДНЫХ И НЕОДНОРОДНЫХ ЭЛЕКТРИЧЕСКИХ ПОЛЯХ В ВОЗДУХЕ

О.В. Мануйленко

Приведены результаты численного моделирования распространения положительного стримера в воздухе в однородных и сильно неоднородных электрических полях. Показано, что динамика распространения стримера в воздухе сохраняет основные черты, характерные для отрицательного стримера в азоте. Показано, что скорость распространения стримера в неоднородном поле больше его скорости в однородном поле при заданных потенциалах на электродах. Показано, что скорость стримера растет с уменьшением радиуса кривизны иглы при заданных потенциалах на электродах. Этот рост продолжается до некоторого критического радиуса, после которого рост скорости положительного стримера практически прекращается.

ЧИСЛОВЕ МОДЕЛЮВАННЯ ДИНАМІКИ ПОЗИТИВНОГО СТРИМЕРА В ОДНОРІДНИХ І НЕОДНОРІДНИХ ЕЛЕКТРИЧНИХ ПОЛЯХ У ПОВІТРІ

О.В. Мануйленко

Наведено результати числового моделювання поширення позитивного стримера в повітрі в однорідних і сильно неоднорідних електричних полях. Показано, що динаміка поширення стримера в повітрі зберігає основні риси, характерні для негативного стримера в азоті. Показано, що швидкість розповсюдження стримера в неоднорідному полі більше за його швидкість в однорідному полі при заданих потенціалах на електродах. Показано, що швидкість стримера зростає із зменшенням радіусу кривизни голки при заданих потенціалах на електродах. Це зростання триває до деякого критичного радіусу, після якого зростання швидкості позитивного стримера практично припиняється.